ISSN 1392–1320 MATERIALS SCIENCE (MEDŽIAGOTYRA). Vol. 28, No. 4. 2022

Thermal and Structural Behaviour of Sandwiched Reinforced Cement Concrete Wall Panels

Ananth THANGARASU *, Jane Helena HENDERSON

Department of Civil Engineering, College of Engineering, Guindy, Anna University, Chennai-600025, India

crossref http://dx.doi.org/10.5755/j02.ms.30339

Received 22 December 2021; accepted 02 March 2022

The energy efficiency of a building predominantly depends on the temperature gradient across the wall. The use of Sandwiched Concrete Panels (SCP) to achieve energy efficiency inside buildings is gaining importance all over the world. This study focuses on comparing the temperature gradient across sandwich concrete wall panels made of two different insulation materials viz. Extruded Polystyrene (XPS) and Expanded Polystyrene (EPS) with two different sizes of steel (8 mm and 10 mm dia.) used as reinforcement and shear connectors. Two different concrete grades viz. M25 and M40 were studied. The thickness of concrete wythes on both sides of the SCP and the inner insulation material (XPS and EPS) were varied to understand their effect on thermal insulation. The external surface of the samples was subjected to an elevated temperature of 75 °C for 24 hours continuously and the temperature measurements across the SCP were recorded. This was done by simulating the real-time temperature effect using an indigenously developed oven, designed and fabricated to fit the SCP sample size which comprises an electronic thermostat and temperature sensor unit arrangement. Additionally, a one-dimensional finite element analysis was carried out to predict the theoretical interface temperature and inner surface temperature of the SCP samples with necessary assumptions. Both the experimental and FEA temperature values corroborated well. Further, all the samples were subjected to compression and flexural testing to evaluate their structural properties. Influence of type of insulation material used viz. XPS and EPS, size of steel reinforcement used viz. 8 mm and 10 mm dia. were found to be not that significant in terms of both thermal and structural behavior.

Keywords: thermal insulation, extruded polystyrene, expanded polystyrene, concrete wythes.

1. INTRODUCTION

In recent times the main research avenues in the construction industry focus on structural integrity, energy efficiency [1], and utility of sustainable materials to gain both economic and environmental benefits without compromising functional efficiency and durability [2]. Among the mentioned three main focuses, developing energy-efficient buildings has attracted researchers globally. The energy efficiency of the building predominantly depends on the temperature gradient across the wall. A higher temperature gradient increases the energy consumption of the building resulting in less energy-efficient buildings [3]. The energy consumption in buildings is nearly 40 % of the total energy consumed in the world and this contributes to 38 % of high pollutant emissions globally [4]. The heat flux entering the building can be reduced by using insulating materials in the building walls [5].

Lightweight Concrete Sandwich Panel walls are widely preferred in high-rise buildings due to their lesser weight and better thermal characteristics [6, 7]. Providing suitable heat transfer control arrangements in the envelope of a building like walls, roofs, and windows, would in turn reduce the energy consumption needed for indoor thermal comfort. Building retrofitting measures is an approach used for reducing energy consumption in existing buildings and in new constructions it can be achieved by using energy-efficient techniques and practices [8]. The optimal energy needed to maintain indoor thermal comfort in a building is best achieved by using appropriate insulating materials during construction. A precast concrete sandwich panel system is one such widely adopted technique to improve energy conservation and efficiency for buildings [9].

In building construction, sandwich panels are generally used as prefabricated or precast concrete components. This precast sandwich wall gained application in the building construction industry due to its improved thermal performance compared to masonry walls and solid concrete panels [10, 11]. The sandwich panels are constructed with two or more layers consisting of high-strength concrete separated by thermal insulating material having low strength. The thickness of the wythes and insulating material depends on application and load-bearing capacity. Kim and Allard [12] studied the thermal response of precast sandwich concrete walls by varying the thickness from 50 mm to 150 mm. Benayoune et.al. [13] found that the optimal thickness of precast reinforced composite sandwich panels that are subjected to axial loading is 38 mm.

The insulation thickness in the concrete composite panel using polystyrene material as insulation agent was studied by Bolattürk [14] and it was found that the optimum range of insulation material thickness lies between 20 to 170 mm. Similarly, an investigation on insulation materials like foam board and polystyrene was conducted by Ucar and Balo [15] and it was reported that the thickness range of insulation material ranges between 10.6 to 76.4 mm to achieve the best performance. Ozel [16] in his study on the

* Corresponding author. Tel.: +91- 9042530546.
E-mail: *anantht@jerusalemengg.ac.in* (A.Thangarasu)

effect of XPS and EPS in building walls, used dynamic thermal analysis and predicted that the optimum thickness of insulation materials falls between 20 to 82 mm. Ekici [17] found that the optimum thickness of the insulation materials like expanded and extruded polystyrene, fiberglass material in different wall assemblies, are in the range of 20 mm to 186 mm. The thermal resistance of the insulation material was only considered in the above works, but the composite concrete panel also plays a vital role in the structural safety of the building which cannot be compromised for any other advantageous impacts.

Hence in this study, a novel attempt is made to predict the appropriate thickness of the insulation element and the corresponding concrete wythes in the composite panel considering the thermal resistance effect and the structural strength. Most preferred insulation materials like EPS and XPS [18 – 23] are taken for this study. M25 and M40 grades of concrete are chosen to cast SCP samples.

Based on the vast literature background, it is evident that both thermal and structural behavior of SCP used in building walls varies with the material type/properties, thickness of the sandwich insulation panel, grade of concrete used, and its size and type and size of shear connectors used. The objectives of this study are:

— to evaluate the temperature at the interface and inner surface locations of SCP samples by subjecting them to an elevated temperature at their external surface using a laboratory oven set-up;
— to calculate the temperature at the different interface and inner surface locations of SCP samples using one-dimensional finite element analysis;
— to investigate the structural behavior of different SCP samples subjecting them to compression and flexure tests as per ASTM standards;
— to identify the best sample combination of SCP samples which would result in providing good insulation behavior without compromising the structural properties.

The overall objective of this study is to identify a suitable Sandwich Concrete Panel (SCP) with robust dimensional parameters and material properties that could resist the impact of extreme temperature on the mechanical/structural behavior of the material and also provide maximum energy efficiency to the building.

2. MATERIALS

A total of 40 different sandwich concrete panels (SCP) and 40 different sandwich concrete panel beams as shown in Table 1 were studied. The total sample thickness is fixed as 150 mm, and only the thickness of composite materials used viz. concrete wythes and XPS/EPS were varied within that 150 mm overall thickness. This size is selected based on detailed literature studies reported and field practices where SCP is generally used as a load-bearing wall or infill wall in buildings. The control samples were cast without any filler material like XPS and EPS. Control samples (CP1 and CP2) for panels of size 500 × 500 × 150 mm and beams of size 700 × 150 × 150 mm were cast for both M25 and M40 grade concretes with steel reinforcements (8 mm and 10 mm dia.) to quantify and understand the percentage reduction in structural strength.

Fig. 1 a shows the longitudinal section of a typical SCP sample of 500 × 500 × 150 mm size with M25/M40 grade reinforced concrete wythes on either side with a sandwiched inner insulating layer made of EPS/XPS material with two diagonal steel shear connectors integrating the composite panel.

Table 1. SCP compression test sample details

S. No.	Thickness, mm			Dia. of reinforcement used, mm	Grade of reinforcement	Grade of concrete used	Insulation material
	Outer concrete	Inner concrete	Insulation Material				
1	50	50	50	8,10 Designated as S1 and S2	550	M25, M40 Designated as C1 and C2	EPS, XPS Designated as X and E
2	55	55	40				
3	60	60	30				
4	65	65	20				
5	70	70	10				

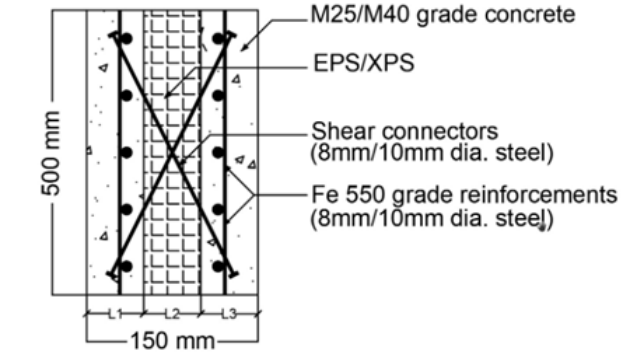

a

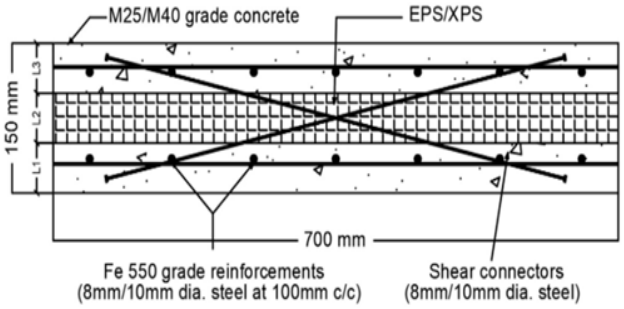

b

c

Fig. 1. Cast specimen: a – typical longitudinal section (LS) (500 × 150 mm with shear connectors); b – LS (700 × 150 × 150 mm with shear connectors); c – SCP samples

Similarly, Fig. 1 b depicts the longitudinal section of a typical SCP beam sample of size 700 × 150 × 150 mm made of two reinforced concrete wythes (M25/M40 grade)

on either side with a sandwiched EPS/ XPS layer, integrated by two diagonal shear connectors. Fig. 1 c shows the 40 SCP samples cast for this study. The properties of cement, fine aggregate, coarse aggregate, and insulation layer used for the preparation of SCP samples are given in Table 2 – Table 5. Concrete mix design had been carried out as per IS 10262-2019 and the mix details are given in Table 6 [24 – 27].

Table 2. Portland pozzolanic cement test properties

Test properties	Cement
Fineness	334 m^2/kg
Initial and final setting time	86 min and 9 hours
Soundness	9.5 mm
Compressive strength (28 days)	35 MPa
Drying shrinkage	0.14 %

Table 3. Fine aggregate properties

Test properties	River Sand
Specific gravity	2.60
Bulk density	1650 kg/m^3
Fine ness modulus	3.12
Water absorption	2.0
Average particle size	1.8 mm

Table 4. Coarse aggregate properties

Test properties	Angular granite
Specific gravity	3.15
Bulk density	2350 kg/m^3
Water absorption	1.06
The average size of aggregate	12 mm

Table 5. Physical properties of EPS and XPS

Properties	EPS	XPS
Density	15 – 30 kg/m^3	15 – 35 kg/m^3
Compressive strength	0.8 – 1.6 kg/m	0.1 – 0.69 kg/m
Tensile strength	3 – 6 kg/cm	3 – 7 kg/cm
Temperature range	- 200 to + 80 °C	- 200 to + 80 °C
Moisture absorption	Very low	Very low
Melting point	General polystyrene melting point is 100 – 248 °C. Above 100 °C the material gets soften	

Table 6. Concrete mix design

Concrete grades	Mix proportion	Water cement ratio	Cement, kg/m^3	Fine aggregate, kg/m^3	Coarse aggregate, kg/m^3
M25	1:1.82:1.68	0.4	445	803.52	741.52
M40	1 :1.33: 2.65	0.35	516	686.0	1367.0

2.1. Experimental investigation

Three specimens were prepared for each of the 40 different SCP samples and all the 120 samples were subjected to testing (Fig. 1 c). After 28 days of curing, all the samples were subjected to a compressive strength test. The test was conducted as per IS 516-2021 standards. The load was applied at the rate of 1mm/min.

Shear connectors used in terms of their quantity provided, arrangement, and reinforcement size play a major role in the mechanical behavior of any SCP [28]. A sandwich composite panel can be considered fully composite only when the two concrete wythes act as a single unit, and this is achieved by providing enough shear connectors between the two wythes [29, 30]. The bending stress distribution of a fully composite panel, partially composite panel, and non-composite panel with two structural wythes and one structural wythe which provides a better understanding of the role of shear connectors in the mechanical behavior of SCP [31 – 34] are shown in Fig. 2.

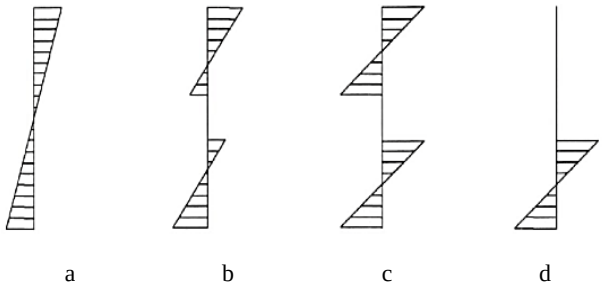

Fig. 2. Stress and strain distribution under flexure: a – fully composite; b – partially composite; c – non-composite, two structural wythe; d – non-composite, one structural wythe

In this study, two diagonally placed steel reinforcement bars of 8 mm and 10 mm size respectively are used as shear connectors (Fig. 3 a).

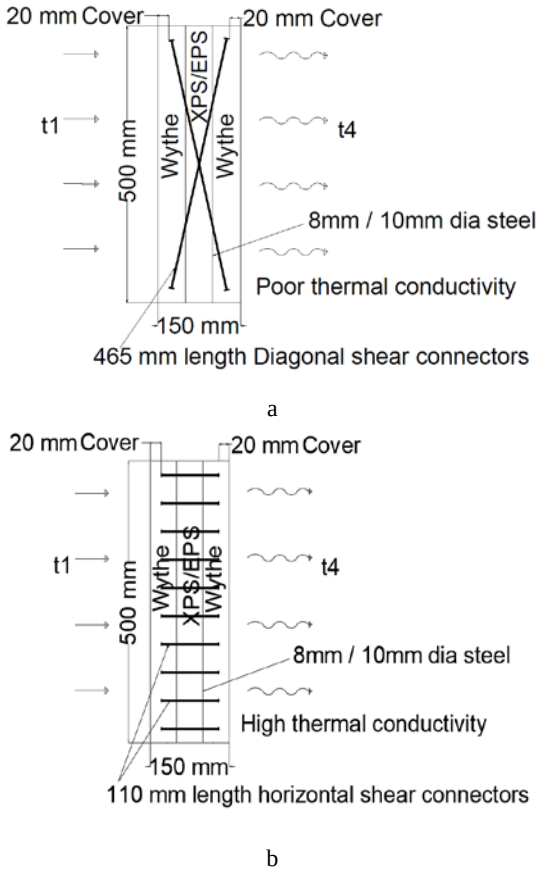

Fig. 3. Arrangement of shear connectors: a – diagonal shear connectors arrangement; b – horizontal shear connectors arrangement

The idea of placing the shear connectors diagonally is to ensure sufficient development length of steel reinforcement on either side of concrete wythes on all 4 corners. This would in turn ensure the required shear connectivity to the sandwich composite panel. A horizontal

shear connector arrangement will result in poor bonding due to the lack of sufficient development length available on either side of the concrete wythe. Also, the thermal conductivity in the SCP will be higher, if multiple horizontal shear connector arrangements are provided as shown in Fig. 3 b.

Fig. 4 a shows the compression test and flexural test on SCP Samples respectively. To check the flexural behaviour of the SCP, a three-point loading flexural strength test was conducted as per ASTM C78/C78M-21 standards on the beam samples. connectors provided. A laboratory-scale heating oven and temperature measuring sensor setup using an electronic thermostat unit were indigenously designed and fabricated for this study to carry out the thermal exposure experiments. This is an attempt to simulate the real-time high-temperature exposure to the SCP covering the buildings all-round particularly in hot regions.

a b

Fig. 4. Mechanical tests on SCP samples: a – compression test; b – flexural test

The electronic thermostat unit includes a temperature sensor, keys, an LED display, and a relay, and it requires a DC 12V power supply. It is a low-cost, high-quality thermostat controller. Thermostats are devices that sense the temperature of a system and keep it at the desired setpoint temperature. The negative temperature coefficient temperature sensor enables the module to control the temperature intelligently. The resistance of the thermistor decreases with increasing temperature because it has a negative temperature coefficient. The electronic thermostat module includes an embedded microcontroller, with a programming set up to evaluate and display the temperature values. The module is made up of three switches that are used to configure the various parameters, such as the ON and OFF trigger temperatures. To turn on, the relay can be powered by voltages as high as 240 V AC at 5 A. The heating range is 0 to 150 °C, and the state is displayed using the 7-segment display and the relay, as well as the LED on the electronic thermostat module. Fig. 5 shows the block diagram of the laboratory scale heating oven developed.

2.2. Simulation of thermal exposure on SCP samples

All the SCP samples were subjected to thermal exposure with their outer walls being exposed/subjected to an elevated temperature (t_1) of 75 °C continuously for 24 hours in the laboratory. The oven used for testing is shown in Fig. 6 a and b. Four temperature monitoring sensors designated as t_{s1}, t_{s2}, $t_{s3,}$ and t_{s4} were used to measure the temperature at various locations as shown in Fig. 6 c.

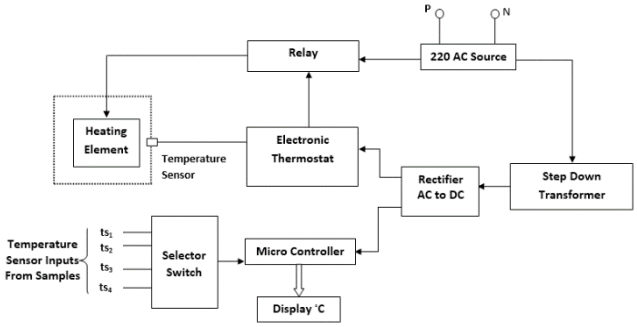

Fig. 5. Block diagram of the laboratory scale heating oven

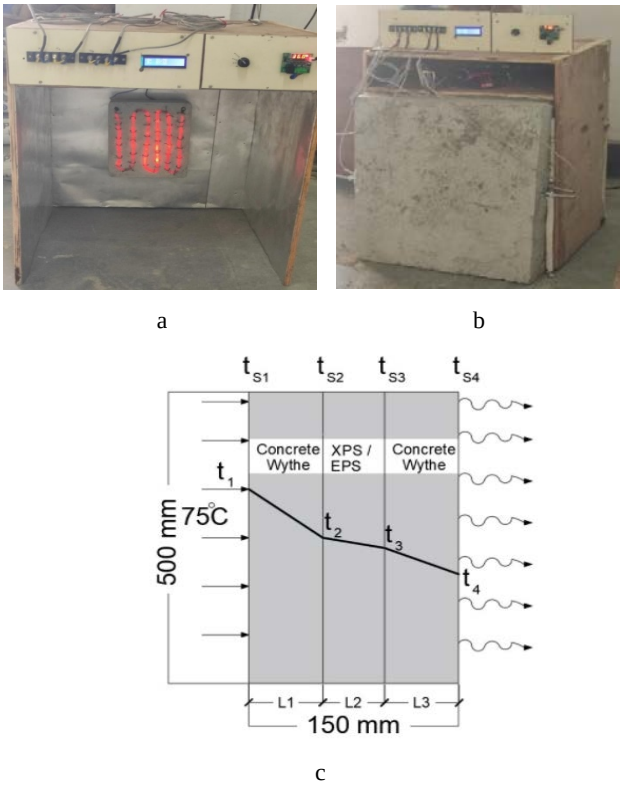

Fig. 6. Details of thermal test: a – interior of oven; b – thermal test in progress; c – schematic representation of the thermal test

The temperature values for all the samples were recorded and tabulated. As temperature exposure is an important factor for condition monitoring of the SCP, it was proposed to fix this high temperature considering the global highest temperature recorded so far. The highest ambient temperature recorded to date is 56.7 °C at Death Valley, California, the USA during July 1913 [35 – 39]. Therefore, in this study, an elevated temperature of 75 °C had been selected for thermal exposure of SCP samples after carefully considering the melting point of the inner sandwiched insulating core polymer material (XPS and EPS) and conducting a series of laboratory trials on the thermal resistance behavior of the samples exposing them to various elevated temperatures.

2.3. Finite element discretization

In this study, one-dimensional Finite Element (FE) analysis is used to predict the interface temperature in the

composite concrete panel with the following assumptions. The thickness of the panel is relatively smaller than its width and height i.e. slightly less than 1/3 of the width and height of the sample.

- There is no heat generation in the panel.
- Contact resistance between the layer is negligible i.e. there is no air gap.
- The thermal conductivity, density, and heat capacity of the material are independent of temperature.
- Differences in the thermal conductivity of M25 and M40 grades of concrete are found to be very negligible. So, thermal conductivity for both types of concrete is assumed to be the same.

The finite element methodology used in this study is clearly shown in Fig. 7.

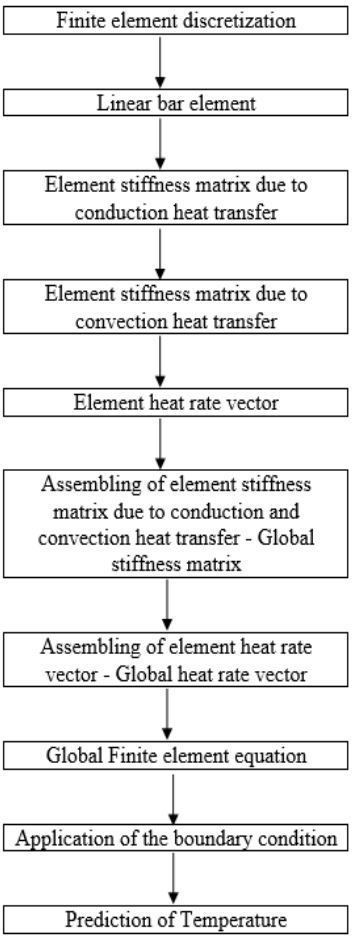

Fig. 7. Flowchart showing Finite element methodology

A composite wall comprising of three layers of different materials is considered as shown in Fig. 8.

The thickness of the different layers is denoted as L_1, L_2, and L_3. The temperature at various points along the cross-section of the composite concrete is designated in finite element analysis as t_1 (exposed temperature in K), t_2 (the temperature at the interface between outer concrete wythe and the insulation material in K), t_3 (the temperature at the interface between the insulation material and the inner concrete wythe in K) and t_4 (the temperature at the inner face of the composite concrete panel in K).

From the inner face of the wall, heat is transferred to the room by convection. The heat from outside enters the building through the exposed external surface of the composite wall by conduction [40, 41]. Steady-state one dimensional heat transfer (q) through the plane wall and the composite wall are given by the Eq. 1 and Eq. 2.

$$q = \frac{kA}{L}(t_1 - t_2) = \frac{t_1 - t_2}{\frac{L}{kA}}, \quad (1)$$

where k is the thermal conductivity; L is the thickness of the wall.

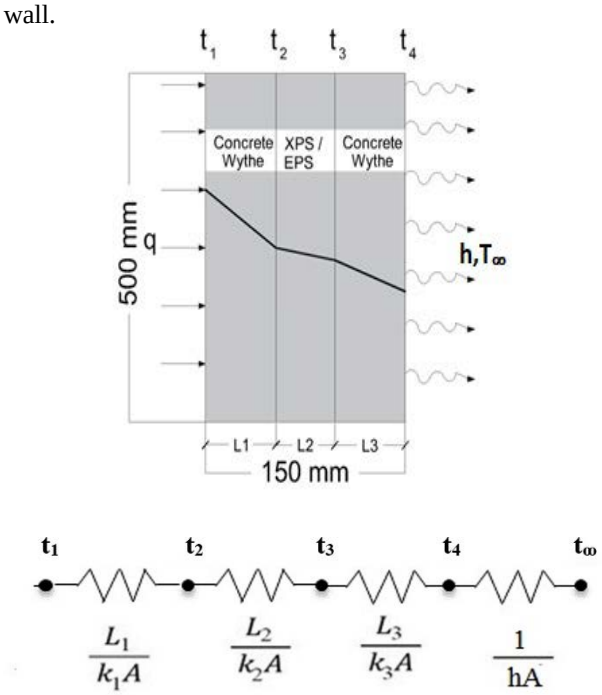

Fig. 8. Heat transfer along the cross-section of SCP Panel with varying thickness

$$q = \frac{t_1 - t_\infty}{\frac{L_1}{k_1 A} + \frac{L_2}{k_2 A} + \frac{L_3}{k_3 A} + \frac{1}{hA}}, \quad (2)$$

where L_1 is the thickness of outer concrete layer of the composite panel in m; L_2 is the thickness of insulation layer of the composite panel in m; L_3 is the thickness of inner concrete layer of the composite panel in m; k_1 and k_3 are the thermal conductivity of inner and outer concrete layer in W/m K; k_1 is the thermal conductivity of the insulation layer in W/m K; t_∞ is the room temperature in K; t_1 is the exposed temperature in K; t_2 is the measured temperature in sleected location in K; h is the convective heat transfer co-efficient in W/m^2 K; A is the area of the cross section of sample in m^2.

The composite wall is subdivided into convenient number of elements. The node and elements are suitably numbered. The equations are derived for each element considering the conduction and convection mode of heat transfer. The heat rate vector is a force vector and is derived by considering heat generation and surface convection. The stiffness matrix for the element with conduction heat transfer is given by Eq. 3 and the heat vector is given by Eq. 4.

Stiffness matrix with conduction heat transfer:

$$[K_c] = \frac{Ak}{L}\begin{bmatrix} 1 & -1 \\ -1 & 1 \end{bmatrix}. \quad (3)$$

The heat rate vector, $\{F\} = \begin{Bmatrix} F_1 \\ F_2 \end{Bmatrix}$. (4)

The stiffness matrix for the element with conduction and convection heat transfer (h) at the end is given by Eq. 5.

$$[K_{c\,h}] = \frac{Ak}{L}\begin{bmatrix} 1 & -1 \\ -1 & 1 \end{bmatrix} + hA\begin{bmatrix} 0 & 0 \\ 0 & 1 \end{bmatrix}. \quad (5)$$

The heat rate vector due to convection at the end is given by the Eq. 6.

$$\{F_h\} = hAT_\infty \begin{Bmatrix} 0 \\ 1 \end{Bmatrix}. \quad (6)$$

The final nodal equation for the outer and middle layer is given by Eq. 7.

$$\frac{AK}{L}\begin{bmatrix} 1 & -1 \\ -1 & 1 \end{bmatrix}\begin{Bmatrix} t_1 \\ t_2 \end{Bmatrix} = \begin{Bmatrix} F_1 \\ F_2 \end{Bmatrix}. \quad (7)$$

Inner layer final nodal equation is given in the Eq. 8.

$$\left\{\frac{Ak}{L}\begin{bmatrix} 1 & -1 \\ -1 & 1 \end{bmatrix} + \begin{bmatrix} 0 & 0 \\ 0 & hA \end{bmatrix}\right\}\begin{Bmatrix} t_3 \\ t_4 \end{Bmatrix} = hAT_\infty \begin{Bmatrix} 0 \\ 1 \end{Bmatrix}. \quad (8)$$

The individual nodal equations are assembled to get a global equation as shown in Eq. 9.

$$\begin{bmatrix} \frac{A_1k_1}{L_1} & -\frac{A_1k_1}{L_1} & 0 & 0 \\ -\frac{A_1k_1}{L_1} & \frac{A_1k_1}{L_1}+\frac{A_2k_2}{L_2} & -\frac{A_2k_2}{L_2} & 0 \\ 0 & -\frac{A_2k_2}{L_2} & \frac{A_2k_2}{L_2}+\frac{A_3k_3}{L_3} & -\frac{A_3k_3}{L_3} \\ 0 & 0 & -\frac{A_3k_3}{L_3} & \frac{A_3k_3}{L_3}+hA \end{bmatrix}$$

$$\begin{Bmatrix} t_1 \\ t_2 \\ t_3 \\ t_4 \end{Bmatrix} = \begin{Bmatrix} F_1 \\ F_2 \\ F_3 \\ hAT_\infty \end{Bmatrix}. \quad (9)$$

The above Eq. 9 is solved to determine the unknown temperature values using the Gauss-Seidal method. To solve the above matrix, the thermal coefficients of various materials as given in Table 7 are used.

Table 7. Input values for different sample types in FEA [36]

S.No.	Entity with unit	Value
1	Thermal conductivity EPS, W/(m·K)	0.042
2	Thermal conductivity XPS, W/(m·K)	0.028
3	Concrete thermal conductivity, W/(m K)	1.74
4	Area of concrete panel, m^2	1
5	Area of insulation thickness, m^2	1
6	Exposed temperature T_1 in K	348
7	Room temperature T_∞ in K	298
8	Convective heat transfer coefficient h, $W/m^2/K$	40

3. RESULTS AND DISCUSSION

The interface temperatures and the temperature at the inner wall surface and the inner side of different SCP samples were evaluated using both an experimental and FE analysis. Table 8 – Table 11 reports the mean temperature values at different locations of SCP samples evaluated during the thermal tests conducted on the samples continuously for 24 hours with thermal measurements taken at every hour interval. Additionally, the room temperature is also measured during this thermal testing which ranges from 22 to 28 °C. Table 12 reports the temperature values evaluated through FE analysis.

Table 8. Temperature values of typical SCP samples with C1 and S1

S.No.	Temp., °C	Control sample	S50		S40		S30		S20		S10	
			X	E	X	E	X	E	X	E	X	E
1	t_2	–	74.61	74.83	74.85	73.92	74.99	73.64	73.57	73.61	72.83	72.07
2	t_3	–	27.73	28.26	28.12	28.59	28.15	28.93	29.03	30.15	33.17	34.73
3	t_4	38.24	26.32	27.19	26.87	27.07	26.95	27.54	28.53	28.82	29.03	29.78

Table 9. Temperature values of typical SCP samples with C1 and S2

S.No.	Temp., °C	Control sample	S50		S40		S30		S20		S10	
			X	E	X	E	X	E	X	E	X	E
1	t_2	–	74.72	74.96	74.89	74.01	75.19	73.85	73.99	74.01	74.03	73.02
2	t_3	–	27.81	28.53	28.27	28.71	28.49	29.02	29.28	30.29	33.49	34.93
3	t_4	38.24	26.41	27.09	26.99	27.13	27.05	27.12	27.72	28.66	30.03	29.98

Table 10. Temperature values of typical SCP samples with C2 and S1

S.No.	Temp., °C	Control sample	S50		S40		S30		S20		S10	
			X	E	X	E	X	E	X	E	X	E
1	t_2	–	74.85	74.88	74.97	73.93	75.05	73.82	74.07	73.83	73.16	72.84
2	t_3	–	27.93	28.76	28.52	28.79	28.56	29.13	29.23	30.34	33.28	34.55
3	t_4	38.29	26.44	27.07	26.17	26.97	26.95	27.83	28.89	29.42	30.15	30.44

Table 11. Temperature values of typical SCP samples with C2 and S2

S.No.	Temp., °C	Control samples	S50		S40		S30		S20		S10	
			X	E	X	E	X	E	X	E	X	E
1	t_2	–	74.92	74.88	74.99	73.92	74.68	73.96	73.89	73.78	74.53	73.59
2	t_3	–	27.56	28.33	28.14	28.67	28.44	28.98	29.13	30.19	33.19	34.78
3	t_4	38.29	26.12	27.04	26.27	27.11	27.75	27.94	28.68	28.99	30.67	30.11

Table 12. Temperature values calculated for SCP using one-dimensional FEA (considering thermal conductivity of C1= C2 and S1 = S2)

S.No.	Temp., °C	Control sample	S50		S40		S30		S20		S10	
			X	E	X	E	X	E	E	X	E	X
1	t_2	–	73.23	73.87	73.95	73.48	73.52	72.87	72.7	71.76	70.65	69.14
2	t_3	–	26.41	27.11	26.86	27.72	27.55	28.68	28.83	30.41	32.05	34.49
3	t_4	36.24	25.65	25.98	25.82	26.20	26.07	26.55	26.54	27.17	27.70	28.64

From the results reported, it is understood that with an increase in sandwich layer thickness (for instance, for 50 mm and 40 mm thickness), there is a significant reduction in temperatures t_3 and t_4. Whereas with a reduction in thickness of the sandwich layer, the concrete wythe thickness increases proportionally and hence the temperatures t_3 and t_4 increase. It is also observed that there are no wide differences in thermal behavior between XPS and EPS and only the thickness of the composite material used has a major impact on thermal insulation behavior. It can also be seen that there is no significant difference in the

temperature values calculated using FE analysis and temperature observed through thermal experiments. Table 8 – Table 11 shows that the t_4 values were different for different concrete grades and thickness of concrete. Hence with an increase in compressive strength, the t_4 values also increase showing a positive correlation between them.

The variation in temperature values observed in thermal tests due to difference in steel reinforcement size viz. 8 mm and 10 mm in SCP is not significant, since the thermal conductivity of steel is the same irrespective of the steel sizes used in this study. Interestingly, significant variations were also not observed due to change in the grade of concrete (i.e. from M25 to M40 grade concrete) used in this study in terms of its thermal conductivity behavior.

Fig 9 – Fig. 13 show the comparison between the temperature values calculated using FE analysis and temperature values observed from thermal tests conducted on one set of SCP samples viz. SX50C1S1 to SX10C1S1 and SE50C1S1 to SE10C1S1 and control samples CP1 and CP2. The comparison of experimental temperature values of different SCP samples with XPS and EPS is shown in Fig. 14 and Fig. 15.

From the plots, a significant temperature difference in the range of 11 to 12 °C can be observed while comparing the t_4 values of the control sample (CP1/ CP2) and SX50 and SE50 type SCP samples, irrespective of concrete grade and steel size. This shows the significance of the thickness of XPS and EPS on the thermal insulation effect.

There is only a slight difference in 't_4'values between SX and SE type samples. This shows that both XPS and EPS exhibited almost identical thermal insulation behavior.

It can also be observed that the temperature gradient/thermal resistance pattern shown by the temperature values t_2, t_3 and t_4 is almost similar in both FEA and thermal tests conducted.

It was found that SX50 and SE50 and SX40 and SE40 samples show better insulation behavior with t_4 values observed in the range of 26 to 27 °C. This sample type, if used could in-turn provide better energy efficiency inside a building.

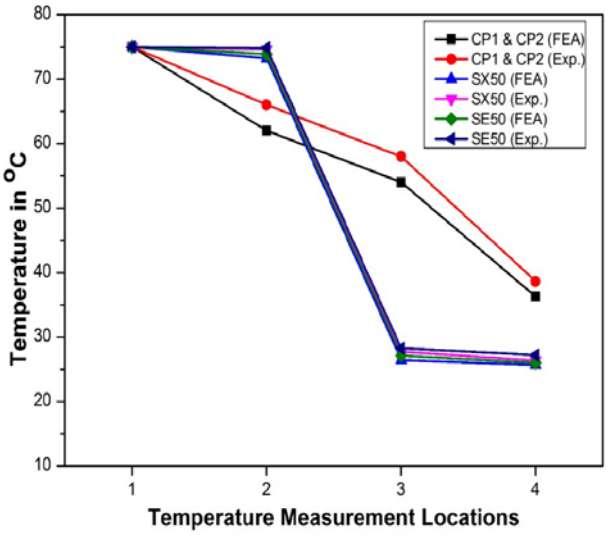

Fig. 9. Comparison of FEA and experimental temperature values (SX50, SE50, CP1 and CP2 samples)

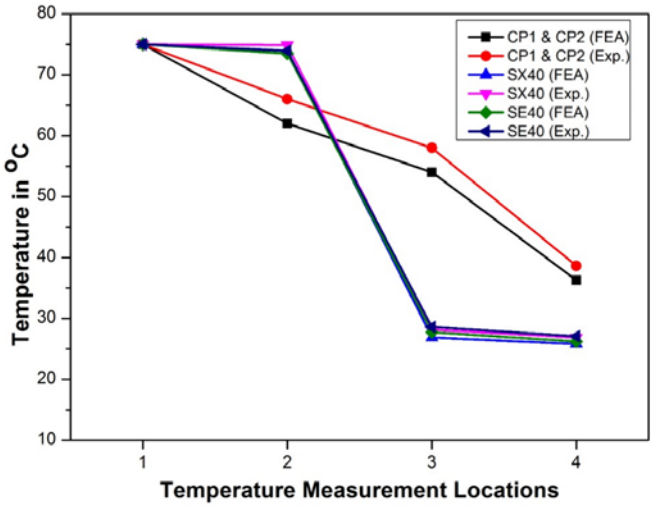

Fig. 10. Comparison of FEA and experimental temperature values (SX40, SE40, CP1 & CP2 samples)

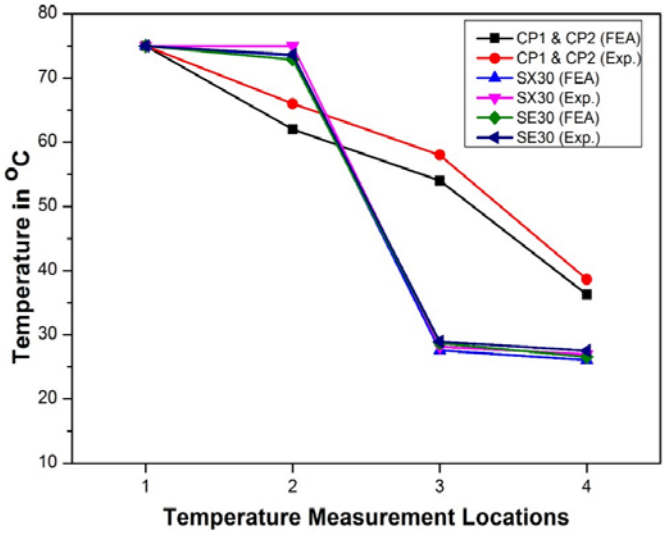

Fig. 11. Comparison of FEA and experimental temperature values (SX30, SE30, CP1 and CP2 samples)

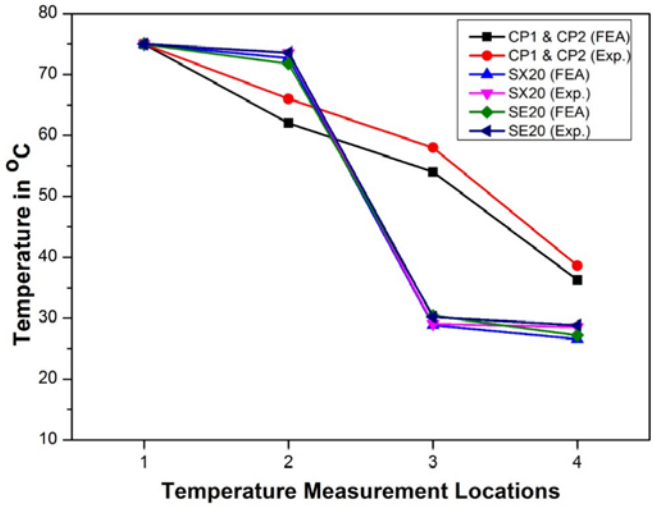

Fig. 12. Comparison of FEA and experimental temperature values (SX20, SE20, CP1 and CP2 samples)

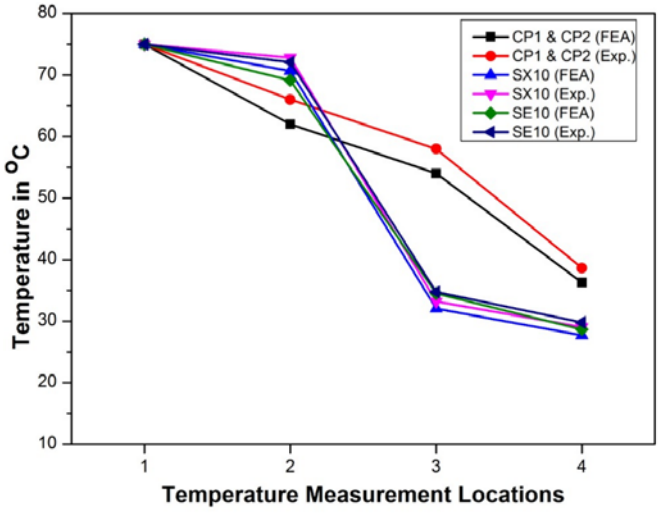

Fig. 13. Comparison of FEA and experimental temperature values (SX10, SE10, CP1 and CP2 samples)

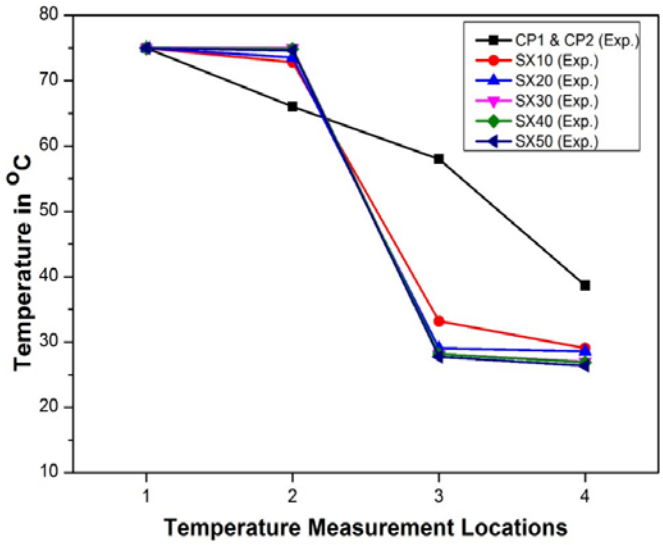

Fig. 14. Comparison of experimental temperature values of different SCP samples with XPS

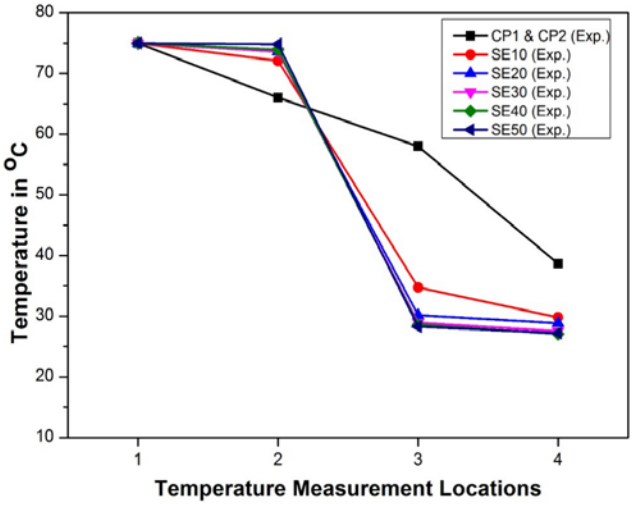

Fig. 15. Comparison of experimental temperature values of different SCP samples with EPS

3.1. Mechanical properties – compressive strength of SCP samples

The crack at the failure of a typical SCP subjected to compression is shown in Fig. 16 a and b below. The crack pattern is seen to be diagonal clearly showing the failure of the sample due to compressive stress. The failure in most of the samples was found to be at the interface between the infill material and concrete wythes. This could be due to a weak bond between two different materials sandwiched together but the integrity of the composite material had been assured by the diagonal shear connector arrangement provided in the sample.

The reports of 28 days compressive strength values of the three replicate SCP samples are shown in Table 13. There is little or no influence of infill insulation material (XPS/EPS) in increasing the compressive strength of the samples whereas with an increase in thickness of the insulation material there is a significant reduction in compressive strength. The compressive strength values of different SCP samples were in close proximity and hence when represented as absolute values in a plot it is difficult to distinguish the impact of concrete grades and sample thickness on the compressive strength. Hence a magnified parameter viz. '% reduction in compressive strength' was used to have a better understanding of the sample's structural behaviour. The % reduction in compressive strength of SCP samples as compared to control samples are calculated using Eq. 10.

$$\%\ \text{Reduction in compressive strength} = \frac{(\text{Compressive strength (Control sample} - \text{SCP sample})}{\text{Compressive strength of Control sample}} \times 100 \quad (10)$$

a

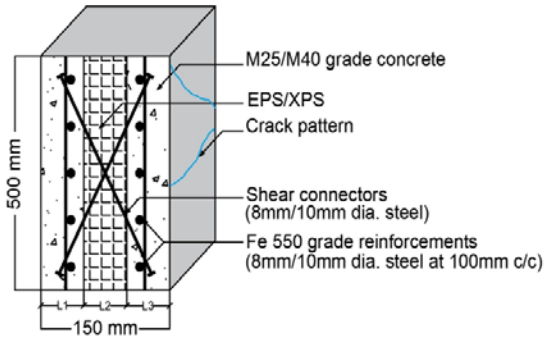

b

Fig. 16. Crack during critical compressive load: a – cracks at failure; b – cracks pattern

Table 13. Compressive strength (N/mm^2) values of different SCP samples

Trials	C1(M25 grade)				C2(M40 grade)			
	S1 (8 mm)		S2 (10 mm)		S1 (8 mm)		S2 (10 mm)	
	SX50	SE50	SX50	SE50	SX50	SE50	SX50	SE50
1	20.33	20.32	20.51	20.50	29.08	29.07	28.04	28.03
2	19.49	19.19	20.37	20.07	29.26	28.96	30.15	29.85
3	19.72	19.52	20.76	20.56	29.30	29.10	31.02	30.82
Mean	19.85	19.68	20.55	20.38	29.21	29.04	29.74	29.57
	SX40	SE40	SX40	SE40	SX40	SE40	SX40	SE40
1	20.06	20.05	21.44	21.43	21.43	30.31	31.13	31.12
2	20.47	20.17	21.39	21.09	21.09	30.42	31.66	31.36
3	20.69	20.49	21.12	20.92	20.92	30.71	32.90	32.70
Mean	20.41	20.24	21.31	21.15	21.43	30.48	31.90	31.73
	SX30	SE30	SX30	SE30	SX30	SE30	SX30	SE30
1	21.10	21.09	23.17	23.16	32.22	32.21	36.97	36.96
2	21.44	21.14	22.39	22.09	34.49	34.19	37.13	36.83
3	22.13	21.93	22.85	22.65	33.28	33.08	37.66	37.46
Mean	21.56	21.39	22.80	22.63	33.33	33.16	37.25	37.08
	SX20	SE20	SX20	SE20	SX20	SE20	SX20	SE20
1	22.85	22.84	23.61	23.60	37.41	37.40	40.36	40.35
2	23.39	23.09	23.50	23.20	36.69	36.39	40.36	40.06
3	23.16	22.96	23.96	23.76	36.90	36.70	41.92	41.72
Mean	23.14	22.96	23.69	23.52	37.00	36.83	40.88	40.71
	SX10	SE10	SX10	SE10	SX10	SE10	SX10	SE10
1	25.35	25.34	27.13	27.12	37.35	37.34	38.66	38.65
2	25.73	25.43	26.88	26.58	37.09	36.79	38.26	37.96
3	25.99	25.79	26.68	26.48	37.68	37.48	37.77	37.57
Mean	25.69	25.52	26.90	26.73	37.37	37.20	38.23	38.06
	CP1				CP2			
1	25.92		26.41		39.04		40.56	
2	27.30		28.84		40.57		39.30	
3	20.33		20.51		29.08		28.04	
Mean	24.52		25.25		36.23		35.97	

There is no difference in compressive strength values due to the change of insulation layer material – XPS and EPS. For instance, in Table 13, it can be observed that the mean compressive strength values of SX50 and SE50 samples of different concrete grade and steel reinforcement combinations are almost similar. Similarly, the difference in compressive strength due to different sizes of steel reinforcement is also not significant. There is only a 7 % difference in compressive strength between M25 grade concrete – 8 mm and 10 mm steel reinforced samples and a 1.5 % difference in compressive strength between M40 grade concrete 8 mm and 10 mm steel reinforced samples.

The compressive strength of the control sample (CP) is around 1.4 to 1.5 times higher than that of sample types SX50/SE50 and SX40/SE40 samples irrespective of concrete grades and reinforcement size. The inner surface temperature (t_4) values achieved by different SCP samples subjected to an elevated temperature of 75 °C at its external surface for a continuous 24 hours period and the corresponding reduction in compressive strength (%) is shown in Fig. 17 a and b respectively.

3.2. Mechanical properties – flexural strength of SCP samples

Flexural strength, also known as bend strength expressed as modulus of rupture provides the maximum amount of tensile load concrete sample can bear before it fails, which means how far the concrete can bend or stretch before failure due to breaking or cracking. It is generally about 10 to 20 % of compressive strength depending on the coarse aggregate used.

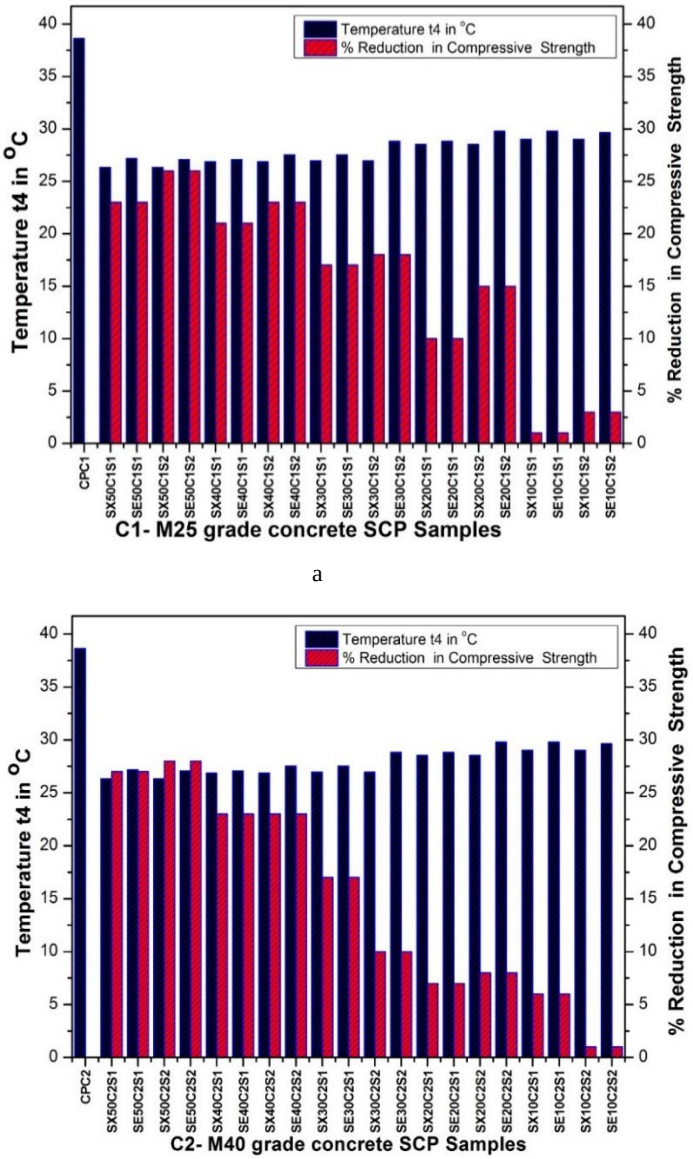

Fig. 17. Temperature t_4 °C and % reduction in compressive strength for M25 and M40 concrete grade SCP samples

The crack pattern at the failure of a typical SCP beam sample subjected to flexural testing in the laboratory is shown in Fig. 18 and the strains are measured at the periphery of the filler. Flexure test crack pattern shows that the crack always develops from the soffit of the beam and progresses towards the center. This shows the integrity of the composite material due to the shear connectors provided. If the composite material lacked structural integrity the cracks might have occurred at the interfaces. Whereas in these samples, the stress transfer from the loading point to the extreme fibre is even which shows the structural integrity of the composite material.

Table 14 reports the 28 days mean flexural strength values of the three replicate SCP beam samples of different types cast for this study purpose and their standard deviation values.

Fig. 18. Cracks at critical flexural load

Table 14. Mean and standard deviation values of flexural strength for different SCP Beam samples

Sample type	Mean values	Standard deviation	Sample type	Mean values	Standard deviation
CPC1S1	3.3	0.23	CPC2S1	4.63	0.11
CPC1S2	3.2	0.62	CPC2S2	3.82	0.11
SX50C1S1	2.82	0.16	SX50C2S1	3.94	0.22
SE50C1S1	2.62	0.24	SE50C2S1	3.70	0.11
SX50C1S2	2.74	0.21	SX50C2S2	3.93	0.22
SE50C1S2	2.50	0.30	SE50C2S2	3.73	0.30
SX40C1S1	2.45	0.27	SX40C2S1	4.30	0.08
SE40C1S1	2.25	0.35	SE40C2S1	4.10	0.05
SX40C1S2	2.72	0.36	SX40C2S2	3.81	0.20
SE40C1S2	2.52	0.46	SE40C2S2	3.61	0.24
SX30C1S1	2.83	0.41	SX30C2S1	4.22	0.60
SE30C1S1	2.63	0.32	SE30C2S1	4.02	0.70
SX30C1S2	3.00	0.35	SX30C2S2	4.41	0.22
SE30C1S2	2.80	0.45	SE30C2S2	4.21	0.21
SX20C1S1	3.41	0.35	SE20C2S1	4.07	0.51
SE20C1S1	3.21	0.26	SE20C2S1	3.84	0.48
SX20C1S2	3.27	0.28	SX20C2S2	4.31	0.19
SE20C1S2	3.07	0.24	SE20C2S2	4.07	0.21
SX10C1S1	3.84	0.15	SE10C2S1	4.19	0.11
SE10C1S1	3.61	0.30	SE10C2S1	4.05	0.15
SX10C1S2	3.77	0.18	SX10C2S2	4.57	0.09
SE10C1S2	3.57	0.10	SE10C2S2	4.34	0.14

From Table 14 it can be observed that with a reduction in the area of concrete wythes in the SCP beam sample there is a proportional decrease in flexural strength. It can be seen that the infill material type i.e. XPS/EPS has no influence on the flexural strength of samples. But with an increase in thickness of the infill material, the concrete wythes thickness proportionally reduces, resulting in a significant reduction in flexural strength.

The reduction in flexural strength in percentage for all the SCP beam samples compared to control samples are provided by Fig. 19 a and b. Reduction in flexural strength was found to be in the range of 7.0 to 9.1 percent for SX50 and SE50 samples and SX40 and SE40 samples of both M25 and M40 grade concrete with 8 mm and 10 mm dia. steel.

There is little difference between the control samples and sample type SX10 and SE10 in terms of flexural strength. A marginal reduction in strength in the range of 3.3 to 3.8 percent is only observed. Small variations in flexural strength values were observed with a change in the size of steel reinforcement from 8 mm (S1) to 10 mm (S2).

From the thermal experiments and mechanical tests conducted viz. compression and flexural strength tests, it was found that SX50 and SE50 and SE40 and SX40 size samples of both M25 and M40 grade concrete with 8 mm and 10 m steel reinforcements provides better thermal insulation behavior without compromising the required structural strength needed for a building block used in a load-bearing wall structure.

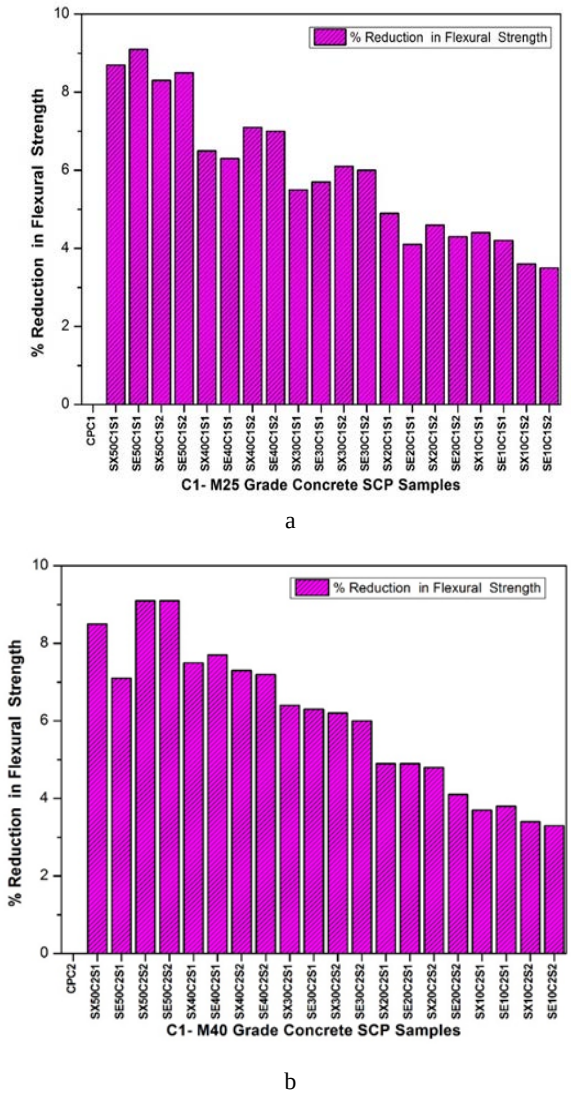

Fig. 19. Reduction in flexural Srength in M25 and M40 grade concrete SCP samples

The compressive and flexural strength of various conventional building blocks are given in Table 15 and it was found that the mechanical properties of SCP samples used in this study – for instance, SX50 and SE50 and SE40 and SX40 are far superior, even after a reduction in structural strength due to the presence XPS/EPS inner insulation core.

Table 15. Compressive and flexural strength of various conventional building blocks (IS:2185 (Part I and II) 1979)

S. No	Material	Compressive strength, N/mm²	Flexural strength, N/mm²
1	Plain cement concrete block	4 – 12.5	0.3 – 0.6
2	Hollow brick block	12.5	0.25
3	Conventional country bricks	4.3 – 5.9	0.2 – 0.3
4	Hollow concrete block	4.0 – 12.0	0.48
5	Solid concrete block	4.0 – 5.0	0.3 – 0.35

For all practical reasons, among these two sample types: SX50 and SE50 samples are the most preferred ones, because of the custom size of the individual elements of this composite panel. For instance, the concrete wythes of SX50 are made up of a standard 50 mm size on both sides and the inner core – XPS insulation material is 50 mm thick. It is easy to cast/manufacture and use this sample size for construction, due to its custom/standard unit size.

For further understanding of the mechanical behaviour of the selected SCP samples SX50 and SE50, the stress vs strain behaviour of these selected SCP samples were studied as per IS 516:2021. The stress is applied on the sample along the axis of loading using a universal testing machine and the corresponding strain response is measured using a DEMEC gauge.

From the stress-strain plots depicted in Fig. 20 and Fig. 21, the following observations were reported.

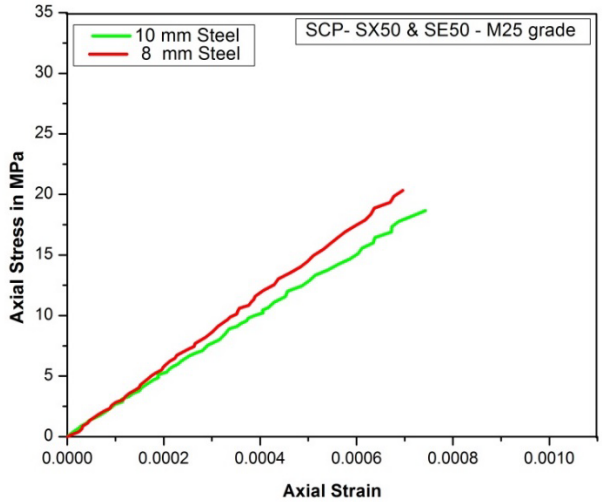

Fig. 20. Stress-strain curves SX50 and SE50 with M25 grade concrete for 8 mm and 10 mm steel reinforcement

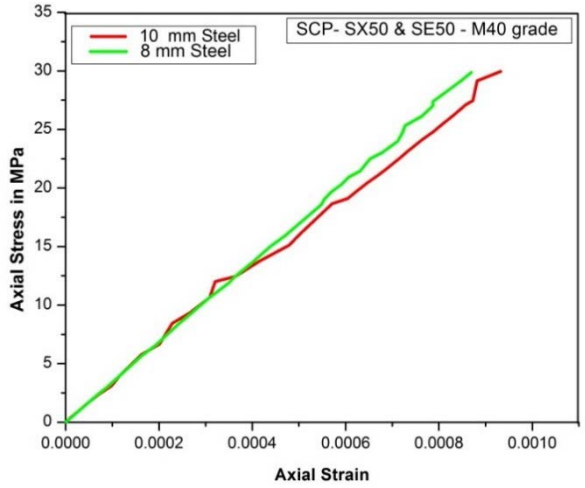

Fig. 21. Stress-strain curves SX50 and SE50 with M40 grade concrete for 8 mm and 10 mm steel reinforcement

Both the plots show that the stress-strain curve increases gradually. Initially, a linear stress-strain behavior is seen in both M25 and M40 grade SCP samples. But overall, the stress-strain relationship shows a non-linear behaviour that follows the typical behaviour of reinforced concrete. With the increase in diameter of steel reinforcement from 8 mm to 10 mm, for the same stress applied, the strain decreases. Similarly, with an increase in grade of concrete i.e., from M25 to M40 grade, for the same applied stress, the strain decreases. This is obviously due to the increased stiffness or modulus.

4. CONCLUSIONS

This study investigated the thermal insulation behavior of different sandwich concrete panels (SCP) by varying the insulation material, concrete grade, steel reinforcement size and sample size combinations.

For this purpose, a laboratory oven set up comprising of an electronic thermostat unit with multiple sensors was indigenously designed, developed and thermal tests were carried out.

A one-dimensional FE analysis was also done to predict the interface temperature and inner surface temperatures of the SCP.

Temperature values evaluated in both thermal tests and FE analysis corroborated well.

Compression tests and flexure tests were carried out to understand the structural behaviour of SCP samples. Beam samples of SCP of size 500 × 150 × 150 mm were cast exclusively for flexural testing.

Thermal and structural tests indicated that SX50 and SX40 SCP of both M25 and M40 grades and 8 mm and 10 mm steel reinforcement provides better thermal insulation without compromising on the required structural strength. The inner surface temperature (t_4) of SX50 and SX40 samples were found to be in the range of 26 °C to 27 °C. This indicates that the thickness of the insulation material (XPS/EPS) has more influence on the thermal insulation behavior.

Reduction in compressive strength of these SCP samples compared to control samples was found to be in the range of 23 to 28 percent. Interestingly, the reduction in flexural strength was found to be only in the range of 7.0 to 9.1 percent.

Hence from this study, it can be concluded that SX50 and SE50 specimens of both M25 and M40 grades and 8 mm and 10 mm steel reinforcement provide good insulation properties, required structural strength and better functional advantage due to its custom size which provides ease in casting and application of SCP on a larger scale as a superstructure building unit.

REFERENCES

1. **Fischer, C., Preonas, L.** Combining Policies for Renewable Energy: Is the Whole Less Than the Sum of Its Parts? *International Review of Energy & Resource Economics* 4 (1) 2010: pp. 51 – 92. https://doi.org/10.1561/101.00000030
2. **Lourenço, L., Zamanzadeh, Z., Barros, J.A., Rezazadeh, M.** Shear Strengthening of RC Beams with Thin Panels of Mortar Reinforced with Recycled Steel Fibers *Journal of Cleaner Production* 194 2018: pp. 112 – 126. https://doi.org/10.1016/j.jclepro.2018.05.096
3. **Pérez-Bella, J.M., Domínguez-Hernández, J., Cano-Sunen, E., Alonso-Martínez, M., del Coz-Díaz, J.J.** Detailed Territorial Estimation of Design Thermal

Conductivity for Façade Materials in North-Eastern Spain *Energy and Buildings* 102 2015: pp. 266 – 276. https://doi.org/10.1016/j.egnbuild.2015.05.025

4. **Simona, P.L., Spiru, P., Ion, I.V.** Increasing the Energy Efficiency of Buildings by Thermal Insulation *Energy Procedia* 128 2017: pp. 393 – 399. https://doi.10.1016/j.egypro.2017.09.044
5. **Berardi, U.** The Impact of Temperature Dependency of the Building Insulation Thermal Conductivity in the Canadian Climate *Energy Procedia* 132 2017: pp. 237 – 242. https://doi.10.1016/j.egypro.2017.09.684
6. **Yu, Q.L., Spiesz, P., Brouwers, H.J.H.** Ultra-light Weight Concrete: Conceptual Design and Performance Evaluation *Cement & Concrete Composites* 61 2015: pp. 18 – 28.

   https://doi.10.1016/j.cemconcomp.2015.04
7. **El Demerdash, I.M.** Structural Evaluation of Sustainable Orthotropic Three-Dimensional Sandwich Panel System. University of California, Irvine, 2013.
8. **Domínguez, S., Sendra, J.J., León, A.L., Esquivias, P.M.** Towards Energy Demand Reduction in Social Housing Buildings: Envelope System Optimization Strategies *Energies* 5 (7) 2012: pp. 2263 – 2287. https://doi:10.3390/en5072263
9. **Mohamad, N., Omar, W., Abdullah, R.** Precast Light Weight Foamed Concrete Sandwich Panel (PLFP) tested under axial load: preliminary results *Advanced Materials Research* Trans Tech Publications Ltd. 250 2011: pp. 1153 – 1162. https://doi.10.4028/www.scientific.net/AMR.250-253.1153
10. **Bai, F., Davidson, J.S.** Analysis of Partially Composite Foam Insulated Concrete Sandwich Structures *Engineering Structures* 91 2015: pp. 197 – 209. http://doi.10.1016/j.engstruct.2015.02.033
11. **Benayoune, A., Samad, A.A.A., Trikha, D.N., Ali, A.A.A., Ashrabov, A.A.** Structural Behavior of Eccentrically Loaded Precast Sandwich Panels *Construction and Building Materials* 20 (9) 2006: pp. 713 – 724. https://doi:10.1016/j.conbuildmat.2005.02.002
12. **Kim, Y.J., Allard, A.** Thermal Response of Precast Concrete Sandwich Walls with Various Steel Connectors for Architectural Buildings in Cold Regions *Energy and Buildings* 80 2014: pp. 137 – 148. https://doi:10.1016/J.ENBUILD.2014.05.022
13. **Benayoune, A., Samad, A.A., Ali, A.A., Trikha, D.N.** Response of Pre-Cast Reinforced Composite Sandwich Panels to Axial Loading *Construction Building Materials* 21(3) 2007: pp. 677 – 685. https://doi10.1016/j.conbuildmat.2005.12.011
14. **Bolattürk, A.** Determination of Optimum Insulation Thickness for Building Walls with Respect to Various Fuels and Climate Zones in Turkey *Applied Thermal Engineering* 26 (11 – 12) 2006: pp. 1301 – 1309. https://doi:10.1016/j.applthermaleng.2005.10.019
15. **Ucar, A., Balo, F.** Effect of Fuel Type on the Optimum Thickness of Selected Insulation Materials for the Four Different Climatic Regions of Turkey *Applied Energy* 86 (5) 2009: pp. 730 – 736. https://doi:10.1016/j.apenergy.2008.09.015
16. **Ozel, M.** Thermal Performance and the Optimum Insulation Thickness of Building Walls with Different Structure Materials *Applied Thermal Engineering* 31 (17 – 18) 2011: pp. 3854-3863. https://doi.org/10.1016/j.applthermaleng.2011.07.033
17. **Ekici, B.B., Gulten, A.A., Aksoy, U.T.** A Study on the Optimum Insulation Thicknesses of Various Types of External Walls with Respect to Different Materials, Fuels and Climate Zones in Turkey *Applied Energy* 92 2012: pp. 211 – 217. https://doi: 10.1016/j.apenergy.2011.10.008
18. **Yu, J., Yang, C., Tian, L., Liao, D.** A Study on Optimum Insulation Thicknesses of External Walls in Hot Summer and Cold Winter Zone of China *Applied Energy* 86 (11) 2009: pp. 2520 – 2529. https://doi:10.1016/j.apenergy.2009.03.010
19. **Fernandes de Oliveira, H., dos Santos Mota, O., Rocha Pinto, F., Barbosa de Alencar, D., Santos Fontineles, F.H., dos Santos Santarém, S., Samuel Dias, Maia, D.** Descriptive Analysis of Advantages and Disadvantages of Expanded Polystyrene Monolytic Panels – EPS *International Journal for Innovation Education and Research* 7 (11) 2019: pp. 159 – 168. https://doi. 10.31686/ijier.vol7. iss11.1867
20. **Ramli Sulong, N.H., Mustapa, S.A.S., Abdul Rashid, M.K.** Application of Expanded Polystyrene (EPS) in Buildings and Constructions: A Review *Journal of Applied Polymer Science* 136 (20) 2019: pp. 1 - 11. https://doi.org/10.1002/app.47529
21. **Fernando, P.L.N., Jayasinghe, M.T.R., Jayasinghe, C.** Structural Feasibility of Expanded Polystyrene (EPS) Based Lightweight Concrete Sandwich Wall Panels *Construction and Building Materials* 139 2017: pp. 45 – 51. https://doi.org/10.1016/j. conbuildmat.2017.02.027
22. **Choi, I., Kim, J., Kim, H.R.** Composite Behaviour of Insulated Concrete Sandwich Wall Panels Subjected to Wind Pressure and Suction *Materials* 8(3) 2015: pp. 1264 -1282. https://doi.10.3390/ma8031264
23. **Selver, E., Gaye, K.A.Y.A.** Low-velocity Impact Behaviour of Carbon/XPS Sandwich Composites *Journal of Textiles and Engineer* 26 (116) 2019: pp. 353 – 359. https://doi:10.7216/1300759920192611607
24. Bureau of Indian Standards for tests for strength of concrete, IS-516, 1959.
25. Bureau of Indian Standards for concrete mix design proportioning, IS-10262, 2009.
26. American Standard for Testing Materials for Flexural Strength of Concrete (Using Simple Beam with Third-Point Loading), ASTM C78/C78M – 21, 2016.
27. **Choi, W., Jang, S.J., Yun, H.D.** Design Properties of Insulated Precast Concrete Sandwich Panels with Composite Shear Connectors *Composites Part B: Engineering* 157 2019: pp. 36 – 42. https://doi.10.1016/j.compositesb.2018.08.081
28. **Choi, K.B., Choi, W.C., Feo, L., Jang, S.J., Yun, H.D.** In-plane Shear Behavior of Insulated Precast Concrete Sandwich Panels Reinforced with Corrugated GFRP Shear Connectors *Composites Part B: Engineering* 79 2015: pp. 419 – 429. https://doi.10.1016/j.compositesb.2018.08.081
29. **Naji, B.** Flexural Analysis and Composite Behavior of Precast Concrete Sandwich Panel *Doctoral Dissertation*, University of Dayton, 2012.
30. **Patil, C.B., Shinde, P.S., Mohite, B.M., Ingale, S.S.** Experimental Evaluation of Compressive and Flexural Strength of Pervious Concrete by Using Polypropylene Fiber *International Journal of Engineering Research & Technology* 6(4) 2017: pp. 756 – 762. https://doi.10.17577/IJERTV6IS040647

31. **Lee, B.J., Pessiki, S.** Thermal Performance Evaluation of Precast Concrete Three-Wythe Sandwich Wall Panels *Energy and Buildings* 38(8) 2006: pp. 1006 – 1014. https://doi:10.1016/j.enbuild.2005.11.014
32. **Vervloet, J., Kapsalis, P., Verbruggen, S., Kadi, M.E., Munck, M.D., Tysmans, T.** Characterization of the Bond Between Textile Reinforced Cement and Extruded Polystyrene by Shear Tests *Multidisciplinary Digital Publishing Institute Proceedings* 2(8) 419 2018: pp. 1 – 6. https://doi.10.3390/ICEM18-05275
33. **Lipczynska, J., West, R.P., Grimes, M., Niall, D., Kinnane, O., O'Hegarty, R.** Composite Behavior of Wide Sandwich Panels with Thin High Performance Recycled Aggregates Concrete Wythes with Fibre Reinforced Polymer Shear Connectors *Journal of Structural Integrity and Maintenance* 6 (3) 2021: pp. 187 – 196. https://doi.org/10.1080/24705314.2021.1906089
34. **Patinha, S., Cunha, F., Fangueiro, R., Rana, S., Prego, F.** Acoustical Behavior of Hybrid Composite Sandwich Panels *Key Engineering Materials* Trans Tech Publications Ltd. 634 2015: pp. 455 – 464. https://doi.10.4028/www.scientific.net/KEM.634.455
35. **Asadi, I., Shafigh, P., Hassan, Z.F.B.A., Mahyuddin, N.B.** Thermal Conductivity of Concrete – A Review *Journal of Building Engineering* 20 2018: pp. 81 – 93. https://doi.10.1016/j.jobe.2018.07.002
36. **Lakatos, A., Varga, S., Kalmar, S.** Influence of the Moisture in the Thermal Conductivity of Expanded Polystyrene Insulators *In book: Contributions to Building Physics* 2 2013: pp. 1 – 4. https://www.researchgate.net/publication/256486555
37. **Kubecka, P.** A Possible World Record Maximum Natural Ground Surface Temperature *Weather* 56 (7) 2001: pp. 218 – 221. https://doi.org/10.1002/j.1477-8696.2001.tb06577.x
38. **Shariq, M., Prasad, J., Mazood, A.** Studies in Ultrasonic Pulse Velocity of Concrete Containing GGBFS *Construction and Building Materials* 40 2013: pp. 944 – 950. https://doi:10.1016/j.conbuildmat.2012.11.070
39. **Lee, J.H., Kang, S.H., Ha, Y.J., Hong, S.G.** Structural Behaviour of Durable Composite Sandwich Panels with High Performance Expanded Polystyrene Concrete *International Journal of Concrete Structures and Materials* 12 (1) 2018: pp. 1 – 13. https://doi.10.1186/s40069-018-0255-6
40. **Seshu, P.** Textbook of Finite Element Analysis, PHI Learning Pvt. Ltd., New Delhi. India, 2003.
41. **Incropera, F.P., DeWitt, D.P., Bergman, T.L., Lavine, A.S.** Fundamentals of Heat and Mass Transfer. Wiley, New York, 6 1996.